Available online at www.sciencedirect.com
ScienceDirect
Journal of Molecular Catalysis A: Chemical 278 (2007) 127–134
JOURNAL OF MOLECULAR CATALYSIS A: CHEMICAL
www.elsevier.com/locate/molcata

Structural studies on a solid self-supported Ziegler–Natta-type catalyst for propylene polymerization

Hanna-Leena Rönkkö [a], Hilkka Knuuttila [a,*], Peter Denifl [b], Timo Leinonen [b], Tapani Venäläinen [a]

[a] *Department of Chemistry, University of Joensuu, P.O. Box 111, FIN-80101 Joensuu, Finland*
[b] *Borealis Polymers Oy, P.O. Box 330, FIN-06101 Porvoo, Finland*

Received 4 June 2007; received in revised form 20 August 2007; accepted 21 August 2007
Available online 2 September 2007

Abstract

The article describes structural studies on a solid $MgCl_2$-based $TiCl_4$ Ziegler–Natta catalyst for propylene polymerization prepared via emulsion technique. Surface area of the catalyst sample was found to be very low. Polymerization activity of the catalyst was nevertheless high. Powder X-ray diffraction (XRD) measurements indicated the presence of δ-$MgCl_2$ in the catalyst sample, and IR and Raman studies the presence of a Mg–Cl bond. Scanning electron microscopy (SEM) measurements revealed an intriguing structure: evidently the catalyst particle is composed of chains (or nanoribbons) that extend from the center of the particle to the surface. SEM measurements further revealed spherical species (diameter about 60 nm) on the surface. Scanning electron microscopy/energy dispersive spectroscopy (SEM/EDS) mappings indicated a high content of titanium evenly distributed throughout the particle, but after moisture treatment of the sample the content was evenly decreased.

Keywords: Ziegler–Natta catalyst; $MgCl_2$; Propylene polymerization; IR; Raman

1. Introduction

Ever since its discovery in the 1950s, the Ziegler–Natta catalyst has played an essential role in the production of polyolefin plastics. The Ziegler–Natta catalysts enable the preparation of polyolefin plastics under conditions of low pressure and temperature. The conventional Ziegler–Natta polypropylene catalyst consists of a $MgCl_2$ support and transition metal component, usually $TiCl_4$ together with the cocatalyst which is usually an aluminum alkyl, such as triethyl aluminum (TEA) or ethyl aluminum dichloride (EADC). Internal and external electron donor compounds are used to control the stereoselectivity. The internal donor is added during the catalyst preparation and the external donor, together with the cocatalyst, to the polymerization reactor [1].

The spherical $MgCl_2$ support for propylene catalysts is prepared in a variety of ways. The methods most widely employed by industry are precipitation and emulsion [2]. Spray crystallization is occasionally used [3,4]. Spray drying and fast quenching methods have been applied as well, but a number of problems remain to be solved (low yield of adduct, fragility, complexity of the process). In the preparation of the $MgCl_2$-supported $TiCl_4$ catalyst, the active component ($TiCl_4$) can be fixed on the $MgCl_2$ support by one of the various methods [5]. Typical methods are impregnation and refluxing for a specific time at a specific temperature [6]. A porous structure with large surface area is obtained.

Ziegler–Natta catalysts for ethylene and propylene polymerization are widely studied and are characterized by many methods. But still, the accurate structure of the catalysts has not been completely solved. Characterization of the structure of a catalyst and the way the catalyst works can offer significant support to catalyst design and development. Also, better control of the polymerization process can be achieved by understanding the relationship between structure and properties of a catalyst. It would be useful to find a relatively easy and quick method of characterization, which indicates, for example, whether the catalyst is active.

* Corresponding author at: Yliopistokatu 7, FIN-80101 Joensuu, Finland. Tel.: +358 13 251 3350; fax: +358 13 251 3390.
E-mail addresses: hanna-leena.ronkko@joensuu.fi (H.-L. Rönkkö), hilkka.knuuttila@joensuu.fi (H. Knuuttila), peter.denifl@borealisgroup.com (P. Denifl), timo.leinonen@borealisgroup.com (T. Leinonen), tapani.venalainen@joensuu.fi (T. Venäläinen).

1381-1169/$ – see front matter © 2007 Elsevier B.V. All rights reserved.
doi:10.1016/j.molcata.2007.08.027

Nitrogen adsorption is recommended and generally used for the study of surface areas larger than 5 m^2/g at low temperature. Argon adsorption is a less common method to measure the adsorption at low temperature. Nitrogen adsorption at 77 K is used to study mesoporous samples and argon adsorption at 87 K to study microporous solids. Brunauer–Emmett–Teller (BET) method is the most common tool for measurement of the surface area of solids [7]. Because the surface area of the present catalyst sample was low, both nitrogen and argon adsorption were applied in measuring the BET surface area.

Electron microscopy is a relatively simple technique for determining particle size and shape and it can even reveal information about the composition and inner structure of a catalyst particle [8]. Scanning electron microscopy (SEM) with elemental analysis was used as an additional technique in the present study.

X-ray diffraction (XRD) is one of the oldest and most widely used techniques for the study of catalysts. XRD is used to identify bulk phases, to describe the kinetics of bulk transformation, and to estimate particle sizes [8]. We used XRD to determine the crystal structure of the catalyst sample and the presence of $MgCl_2$ in the sample.

The use of IR spectroscopy in the characterization of heterogeneous Ziegler–Natta catalysts has intensified in recent years. The most intensely studied region in the IR spectra of catalyst samples is 1800–1600 cm^{-1}, where the frequency of νC=O (internal electron donor) appears. The far-IR region is also important, where the signals of metal–chloride and metal–oxygen bonds occur. Interpretation of the far-IR region is not easy, however, especially for $MgCl_2$-supported catalysts, because the characteristic signals of the catalyst complex tend to be weak compared with the vibrational transitions of $MgCl_2$. Raman spectroscopy is less often used in catalyst characterization. However, the Raman spectra of $MgCl_2$-supported Ziegler–Natta catalysts are relatively easy to interpret, and the signals of $TiCl_4$ and $MgCl_2$ can be isolated [9,10]. Raman spectroscopy might therefore be a more useful technique than IR spectroscopy to study the $MgCl_2$-based Ziegler–Natta catalyst. In this work we were interested in the signals of Mg–Cl and Ti–Cl bonds and metal–oxygen bonds.

The methods described above were applied to elucidate the structural features of a solid self-supported Ziegler–Natta-type polypropylene catalyst prepared by an emulsion technique patented by Borealis Polymers Oy [11]. The emulsion technique represents a unique approach to the preparation of polymerization catalysts. In conventional polypropylene catalysts the active species are fixed to the solid support, whereas in studied catalyst the solid support is formed during the catalyst preparation process as an integral part of the catalyst particle. The catalyst can thus be described as self-supported. Traditionally, the Ziegler–Natta catalyst has a large surface area, which is thought to be the prerequisite for high-polymerization activity. The surface area of studied catalyst was exceptionally low, but still the activity of the catalyst was very good.

2. Experimental

2.1. Preparation of solid catalyst

The catalyst was synthesized by a novel emulsion method developed by Borealis Polymers Oy. Main reactions of the catalyst preparation are presented in Scheme 1. The first stage of the preparation consisted of in situ formation of a liquid/liquid two-phase system where one phase was a solution of the catalyst components in an inert solvent. In the first step of stage 1, butyl octyl magnesium (BOMAG) and 2-ethyl-1-hexanol were reacted to magnesium alkoxide. In step 2 the magnesium alkoxide (formed in step 1) was allowed to react with phthaloyl dichloride (PDC) at 60 °C and the $MgCl_2$/DEHP complex was formed. Di(ethylhexyl)phthalate (DEHP) is also known as di(octyl)phthalate (DOP). In step 3 the $MgCl_2$/DEHP complex was reacted with $TiCl_4$ and a liquid/liquid two-phase system was formed. In the second stage the catalyst droplets were stabilized through an addition of surfactant (emulsification). The final stage, solidification of the catalyst droplets, was achieved by changing the reaction conditions of the emulsion system. The catalyst particles were then isolated and dried [11].

2.2. Polymerizations

The propylene bulk polymerizations were carried out in a stirred 5-l tank reactor in Borealis Polymers' catalyst laboratory. The cocatalyst was triethyl aluminum (TEA) and the external donor cyclohexyl methyl dimethoxy silane (CMMS). Al/Ti mole ratio and Al/CMMS mole ratio were 250 mol/mol and 10 mol/mol, respectively. In the polymerization the cocatalyst, external donor, and 30 ml *n*-pentane were first mixed and allowed to react for 5 min. Half of the mixture was then added to the polymerization reactor and the other half was mixed with about 20 mg of catalyst. After an additional 5 min, the catalyst/TEA/donor/*n*-pentane mixture was added to the reactor. Seventy-millimole hydrogen and 1400 g propylene were introduced into the reactor and the temperature was raised within ca. 15 min to 70 °C. The polymerization time after reaching polymerization temperature was 60 min.

2.3. Characterization methods

2.3.1. BET method

Surface area of the catalyst sample was determined by Brunauer–Emmett–Teller (BET) method via nitrogen adsorption and argon adsorption. The instrument was a Micromeritics ASAP 2010. Both N_2 gas and Ar gas were used at their liquefaction temperatures (77 K and 87 K, respectively). Samples were handled and packed to the analysis tubes under nitrogen atmosphere and the surface area measurements were carried out inertly.

2.3.2. Scanning electron microscopy

A high-resolution Hitachi S4800 field emission scanning electron microscope was used in the scanning electron

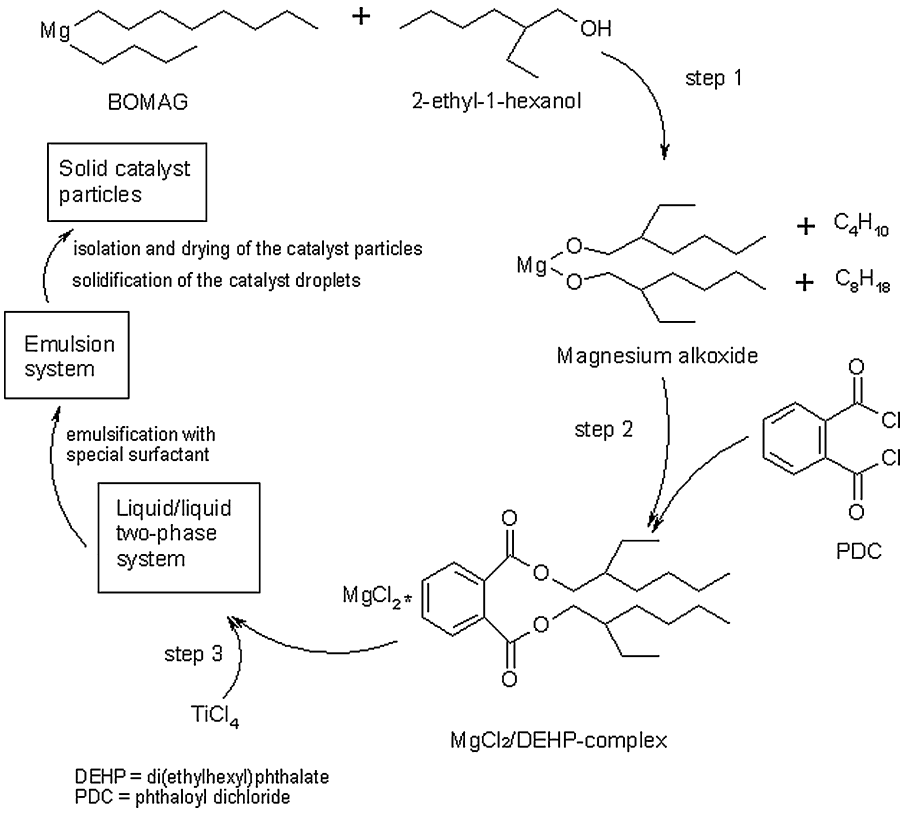

Scheme 1. Main reactions of the catalyst preparation.

microscopy (SEM) measurements. The catalyst sample was preserved under nitrogen atmosphere. Before the measurements the sample was quickly fixed on a glue-covered tape and then quickly moved to the loading chamber of the electron microscope. Voltage and the working distance varied during the measurements as noted on the SEM photographs.

The energy dispersive spectroscopic analyses (SEM/EDS) were done in the laboratory of Borealis Polymers Oy. The SEM equipment was a JEOL 840 and the EDS equipment a Princeton Gamma-Tech (PGT) with Omega detector.

2.3.3. Powder X-ray diffraction measurements

The instrument used for the powder X-ray diffraction measurements was a Bruker AXS, D8 Advance X-ray diffractometer. The catalyst sample was placed on the special sample holder made of stainless steel, and the holder was sealed with a thin Mylar film of 3.6 μm so that the measurement could be performed inertly. The step size in the XRD measurements was 0.04° and the time per step was 8 s.

2.3.4. Infrared spectroscopy

The mid-IR spectra of the catalyst samples were measured using a Nicolet Impact 400 D infrared spectroscope. The equipment was mounted inside a glove box so that samples could be measured by inert diffuse reflectance infrared Fourier transform (DRIFT) method. The measuring range was 4000–650 cm^{-1}.

Far-IR spectra were measured at the University of Helsinki (Department of Inorganic Chemistry) with a Perkin-Elmer Spectrum GX spectroscope. Measurements were carried out in the area 30–710 cm^{-1} but the area reported was defined between 200 cm^{-1} and 650 cm^{-1} because the most important vibrations can be assumed to occur in this area, and below 200 cm^{-1} the noise was too disruptive. Far-IR measurements were performed by two methods: in KBr and in Nujol mull on polystyrene film. The both methods gave similar results.

2.3.5. Raman spectroscopy

Raman measurements were carried out using red (633 nm), green (515), and UV (325 nm) lasers at the Mikkeli Technology Center on Jobin Yvon Horiba HR 800 UV equipment. Samples were packed in quartz glass capillaries in nitrogen atmosphere. Unfortunately, catalyst samples were destroyed during the measurements (with all lasers mentioned above). Subsequently, samples were however successfully measured with the FT-Raman spectrometer RFS100/S from Bruker Optics GmbH, using a laser of 1064 nm. Fluorescence was corrected with the concave rubberband correction method.

2.3.6. Moisture treatment of the catalyst sample

The catalyst sample was treated with toluene of known moisture content to study the effect of moisture on the catalyst structure. The moisture content in toluene was 120 ppm. After the moisture treatment the sample was studied by SEM and SEM/EDS, and elemental analysis was carried out.

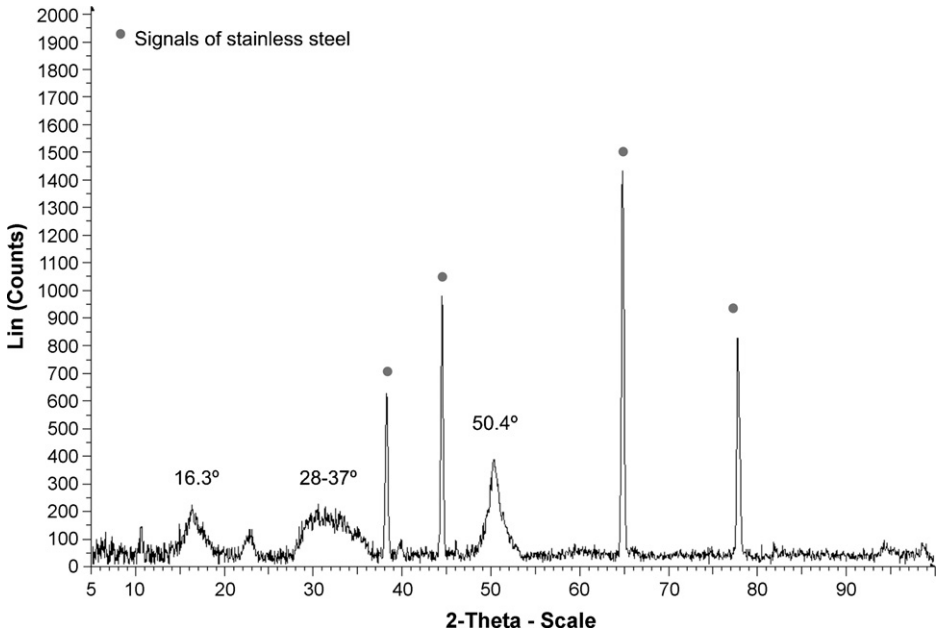

Fig. 1. Powder X-ray diffractogram of the catalyst sample.

3. Results and discussion

3.1. Polymerization activity

The catalyst characterized in this study obtained activity of 23.1–35.5 kg PP/(g cat h) in propylene bulk polymerization. Melt mass-flow rate (230 °C/2.16 kg) was in the range of 4–5.8 g/10 min and xylene solubility was 1.4–1.5 wt%.

3.2. Catalyst morphology and inner structure

The surface area of the catalyst sample was determined with use of both nitrogen (77 K) and argon (87 K) gases. The results obtained with the two gases were similar: the surface area was only about 2 m^2/g, which is an exceptionally low value for a polymerization catalyst. The corresponding value of the reference catalyst (conventional $MgCl_2$-supported PP catalyst) may be 300 m^2/g or more [12].

The powder X-ray diffractogram of the catalyst sample is presented in Fig. 1. Signals at 16.3°, 28–37°, and 50.4° and the profiles of those signals correspond to structurally disordered δ-$MgCl_2$, while the signals at the 2θ values of 38.3°, 44.5°, 64.7°, and 77.8° are due to the stainless steel sample holder. The signal at about 16.3° is related to the stacking of Cl–Mg–Cl triple layers along the crystallographic direction. Signals at 28–37° and 50.4° are related to stacking faults in the triple layers [13,14].

The primary interest in the IR and Raman measurements was the signals of the Ti–Cl, Mg–Cl, Ti–O, and Mg–O bonds. Also, the signals of the electron donor were studied. Fig. 2 presents the mid-IR spectrum and Fig. 3 the far-IR spectrum of the self-supported catalyst sample. The Raman spectrum of the same sample is presented in Fig. 4. The characteristic IR and Raman vibrations are collected in Table 1. The typical signals of the alkyl groups are seen in the mid-IR (Fig. 2) and Raman (Fig. 4)

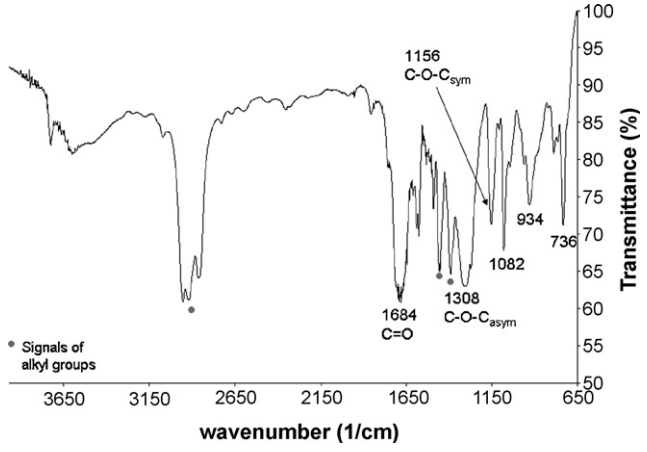

Fig. 2. Mid-IR spectrum of the self-supported catalyst sample.

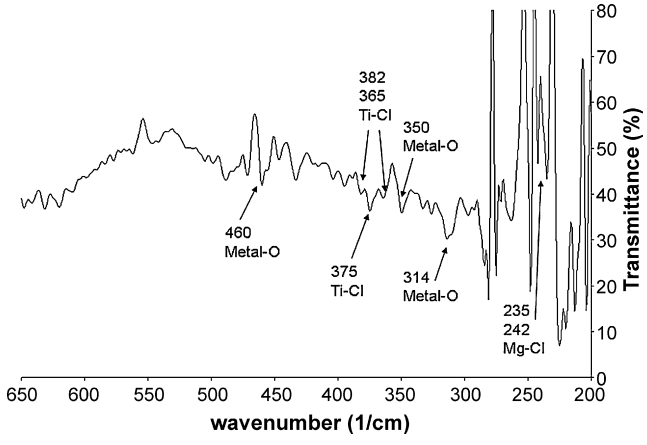

Fig. 3. Far-IR spectrum of the self-supported catalyst sample.

Table 1
Characteristic IR and Raman vibrations of the catalyst sample

Vibration	Type of vibration	Region (cm^{-1})	
		IR	Raman
$C–H_{Ar}$	Stretching	3070	3080
CH_2/CH_3	Stretching	2800–3000	2800–3000
C=O	Stretching	1684	1685
$C=C_{Ar}$	Stretching	–	1592
CH_2/CH_3	Deformation vibration	1454	1449
CH_3	Symmetric deformation vibration	1392	1395
C–O–C	Asymmetric stretching	1308	1302
C–O–C	Symmetric stretching	1156	1156
$C–H_{Ar}$	In plane deformation vibration	–	1140
O–C=O	Asymmetric stretching	1082	–
$C–H_{Ar}$	In plane deformation vibration	–	1052
O–C=O	Symmetric stretching	934	–
C–H	Out of plane deformation vibration	736	647
M–O (Mg–O or Ti–O)	Stretching	460	–
Titanium compound	Stretching	–	419
M–O (Mg–O or Ti–O)	Stretching	350	350
M–O (Mg–O or Ti–O)	Stretching	314	303
Ti–Cl	Stretching	375	–
Ti–Cl	Stretching	365	–
Ti–Cl	Stretching	382	–
Mg–Cl	Stretching	233	238
Mg–Cl	Stretching	242	–

spectra of the catalyst sample. The signal at 3080 cm^{-1} with strong intensity in the Raman spectrum and weak intensity in the mid-IR spectrum is due to the stretching vibration of the ring C–H bonds [15]. The mid-IR spectrum (Fig. 2) shows a signal at 736 cm^{-1} due to the aromatic out-of-plane C–H deformation vibrations and ring out-of-plane vibrations, indicating that the aromatic ring is 1,2-disubstituted. No signal appears in the area 660–730 cm^{-1}, indicating that the substituents are identical (IR inactive). The Raman spectrum (Fig. 4) exhibits a strong signal at about 650 cm^{-1} due to the ring vibrations. The weak signals at 1492–1555 cm^{-1} in the mid-IR spectrum are due to aromatic C=C stretching vibrations, and the doublet at 1578 cm^{-1} and 1591 cm^{-1} is due to aromatic ring where C=O is directly conjugated to the ring. The signal at 1592 cm^{-1} in the Raman spectrum (Fig. 4) is due to aromatic C=C stretching vibrations. Often this is the strongest signal of the Raman spectrum [15].

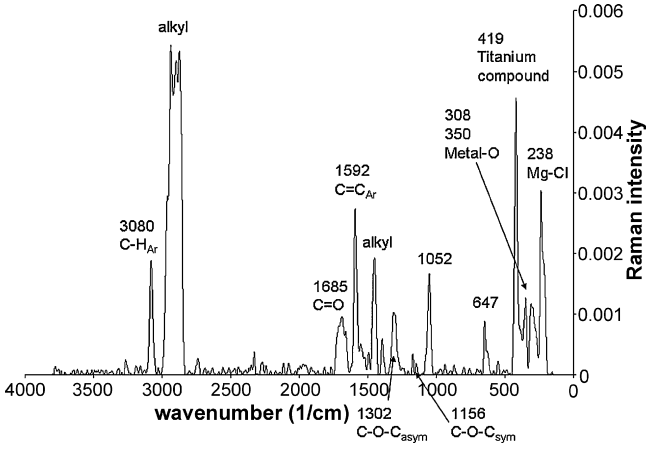

Fig. 4. Raman spectrum of the self-supported catalyst sample.

The intense signal at 1684 cm^{-1} in the IR spectrum (Fig. 2) and the weak signal at 1685 cm^{-1} in the Raman spectrum (Fig. 4) are due to the C=O stretching vibrations of the carbonyl group of the ester. The signals of the asymmetric and symmetric stretching vibrations of C–O–C are present in the IR spectrum of the catalyst sample (Fig. 2) at 1308 cm^{-1} and 1156 cm^{-1}, respectively, with strong intensity. In the Raman spectrum (Fig. 4) these signals exist at 1302 cm^{-1} and 1156 cm^{-1} with medium and weak intensities, respectively. The signal at 1044 cm^{-1} with weak intensity in the IR spectrum and at 1052 cm^{-1} with medium intensity in the Raman spectrum is due to the ring stretching vibrations.

The far-IR spectrum of the catalyst sample (Fig. 3) shows a signal at 242 cm^{-1} due to the Mg–Cl bond. There is also a signal at 235 cm^{-1} in the IR spectrum and at 238 cm^{-1} in the Raman spectrum (Fig. 4), which may be due to the Mg–Cl bond [16]. A strong signal at 243 cm^{-1} can also be found in the Raman spectrum of $MgCl_2$ (Fig. 5, measured with UV-laser). The signal at 375 cm^{-1} in the IR spectrum of the catalyst sample is due to the Ti–Cl bond, where Cl is terminal and the titanium is six-coordinated. The shoulders at 365 cm^{-1} and 382 cm^{-1} are also due to the terminal Ti–Cl bond [15]. The signal at 419 cm^{-1} in the Raman spectrum of the sample (Fig. 4) is the signal of the titanium compound [17]. The Raman spectrum of the catalyst sample also shows signals at 308 cm^{-1} and 350 cm^{-1}, which appear in the far-IR spectrum at 314 cm^{-1} and 350 cm^{-1}. These probably are the signals of the metal–oxygen bond (Mg–O or Ti–O).

The optical microscope image of the catalyst sample (Fig. 6) shows the catalyst particles to be of perfectly spherical shape,

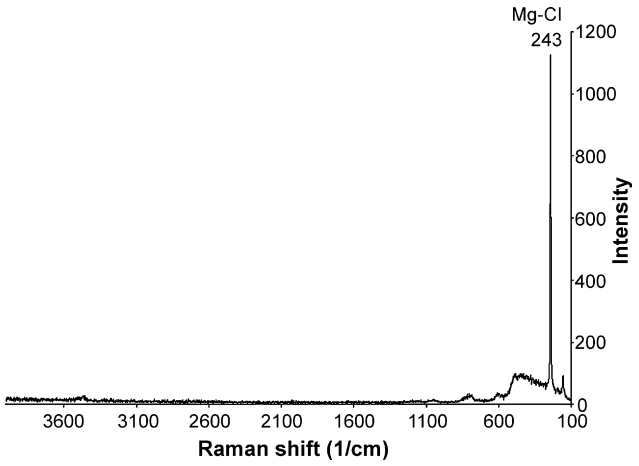

Fig. 5. Raman spectrum of $MgCl_2$.

about 20 μm in diameter. None of the particles were agglomerated. The accurate high-resolution SEM micrographs of the catalyst particle revealed spherical surface species about 40–60 nm in diameter. Further, SEM measurements revealed a chain-like inner structure of the particles, where the chains extend from the center of the particle to the surface. This is clearly seen in Figs. 7–9. An SEM photograph of the surface species of the catalyst particle is presented in Fig. 10.

Several studies [18–21] have suggested that $MgCl_2B_x$ adducts (B = Lewis base) consist of $MgCl_2$ polymeric chains. The authors propose that the δ-form of $MgCl_2$ (obtainable by complete elimination of Lewis base from the adduct) consists of a large number of covalent $[MgCl_2]_n$ polymeric chains. In agreement with this, our self-supported catalyst consists of polymeric nanoribbons of $MgCl_2$ to which titanium active centers and internal electron donor are attached. In addition to the signals of δ-$MgCl_2$ appearing in the powder XRD measurements, the presence of $MgCl_2$ in the catalyst was indicated by the signals of the Mg–Cl bond in IR and Raman spectra.

Chang et al. [22] have detected a similar inner structure for a PP catalyst prepared by a precipitation method. They prepared microcrystal particles of $MgCl_2$ by dissolving a mixture of complexes of anhydrous $MgCl_2$ with epichlorohydrin and tributyl phosphate in toluene and then removing the organic components from the $MgCl_2$ complexes with excess of $TiCl_4$. Solid support particles of microspherical form were obtained after heating.

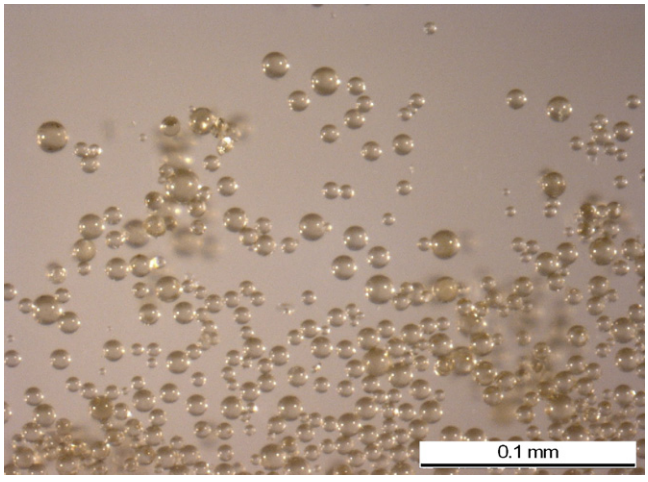

Fig. 6. Optical microscope image of the catalyst particles.

Fig. 7. SEM photograph of the catalyst particles.

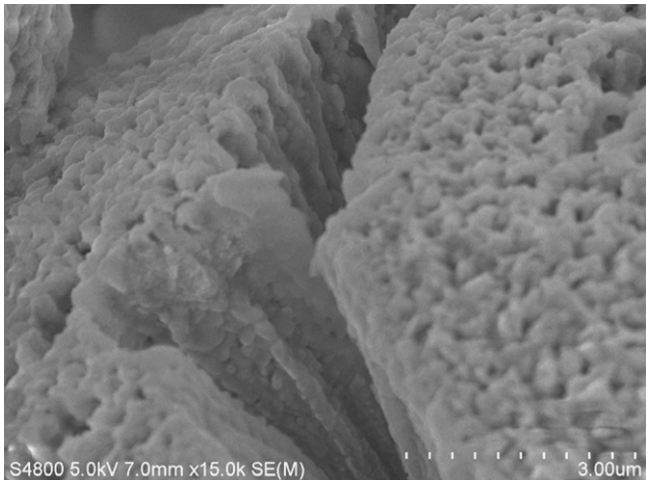

Fig. 8. SEM photograph of the catalyst particle.

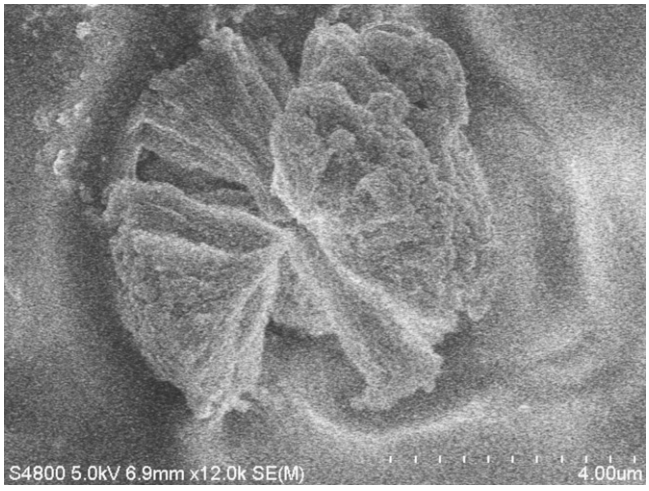

Fig. 9. SEM photograph of the ruptured catalyst particle.

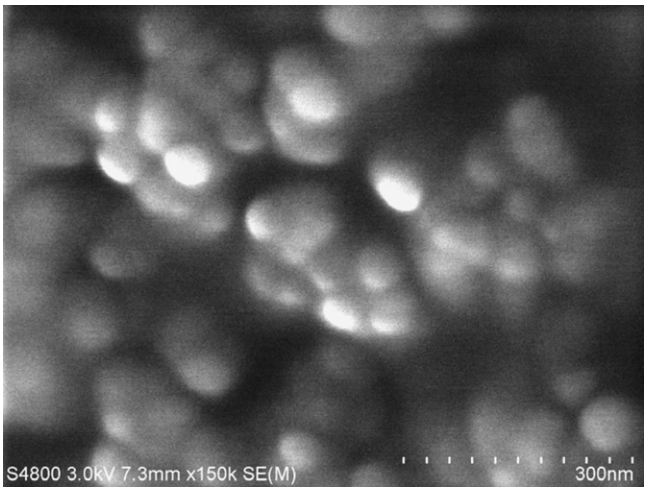

Fig. 10. SEM photograph from the surface of the catalyst particle.

The authors report a "sea urchin"-type crystallite structure for the catalyst particles: particles are tightly filled with long rods of $MgCl_2$ crystallites, and the planes of the Cl–Mg–Cl crystal layers are directed perpendicular to the lengths of the rods. However, according to SEM pictures the morphology of the catalyst particles suggests agglomerates of several spherical primary particles.

To reiterate, studied catalyst particles are non-agglomerated and filled with δ-$MgCl_2$ nanoribbons. Titanium active centers and internal donors are coordinated to these ribbons, creating a porous structure inside the catalyst particle. BET measurements showed that the catalyst is characterized by exceptionally low mesoporosity, while the powder XRD and SEM pictures together revealed a porous δ-$MgCl_2$ crystallite structure. SEM/EDS mappings revealed good distribution of titanium throughout the particle (Fig. 11). The catalyst was highly active in propylene polymerization (35 kg PP/(g cat h)), and evidently, because of this exceptional structure, the monomer does not encounter a diffusion problem in the polymerization.

3.3. Moisture treatment of the catalyst sample

Despite the low mesoporosity and low surface area of studied self-supported catalyst, the polymerization activity was good. SEM/EDS studies on cross-sections of the catalyst particles showed a highly even distribution of titanium through the particle indicating homogeneous structure of the catalyst particles.

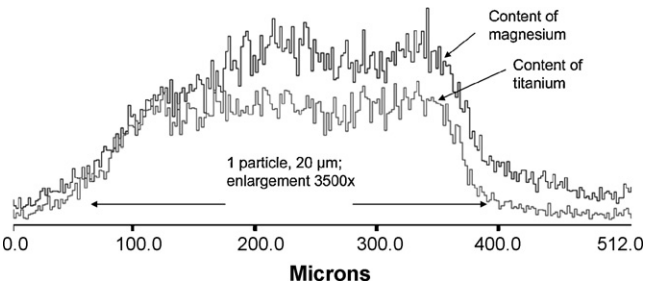

Fig. 11. SEM/EDS mapping of the catalyst particle.

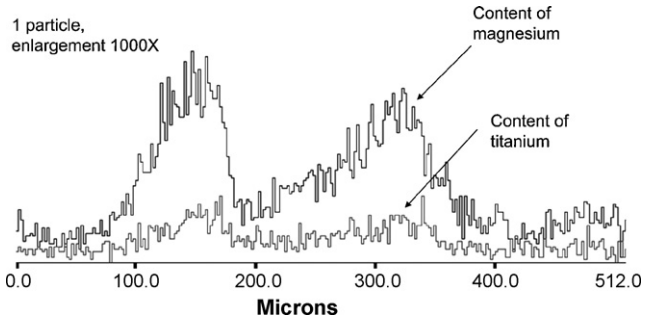

Fig. 12. SEM/EDS mapping of the catalyst particle after moisture treatment.

SEM/EDS mapping (Fig. 12) of particles that had been treated with wetted toluene (120 ppm) further indicated an even loss of titanium from the whole particle. Even though the surface area and pore volume of the particles are very small, the titanium appears able to disengage evenly from the catalyst particle. The unique inner structure of the catalyst sample (nanoribbons) may explain why the titanium was capable of being consumed evenly.

4. Conclusions

A solid self-supported Ziegler–Natta-type catalyst for propylene polymerization was studied and characterized by various methods. BET measurements with nitrogen and argon revealed an exceptionally low surface area and low mesoporosity, especially compared with that of the conventional $MgCl_2$-based Ziegler–Natta-type catalyst for propylene polymerization. Despite the low mesoporosity and low surface area of the catalyst, the polymerization activity was good.

Powder XRD measurements indicated the presence of δ-$MgCl_2$ nanoribbons in the catalyst structure, and IR and Raman spectroscopies the presence of Mg–Cl bond. High-resolution SEM micrographs revealed spherical surface species about 40–60 nm in diameter, and also a chain-like structure within the catalyst particles, with the chains extending from the center of the particle to the surface. Evidently, because of this exceptional structure, the monomer does not encounter diffusion problems in the polymerization.

According to the IR characterization of the catalyst samples it seems that the active titanium centers and internal donors are coordinated to these $MgCl_2$ nanoribbons, creating a porous structure inside the catalyst particle. SEM/EDS mappings revealed that the titanium content is high and the titanium is evenly distributed through the particle. Moisture treatment decreased the content of titanium evenly. Even though the structure of the catalyst appeared compact, the titanium was capable of disengaging evenly from the whole particle. The explanation for this may be the chain-like inner structure of the catalyst particle.

Acknowledgments

Our thanks to Borealis Polymers Oy (Finland) for funding the research and supplying the catalyst samples, to Mikkeli Technology center and Bruker Optics GmbH for the Raman

measurements, and to the Department of Inorganic Chemistry, University of Helsinki, for putting the far-IR equipment at our disposal. Valtteri Kalima is thanked for taking the high-resolution SEM pictures.

References

[1] F.J. Karol, Polym. Mater. Sci. Eng. 80 (1999) 277.
[2] G. Collina, D. Evangeliste, M. Sacchetti, WO Patent 2005/063832 A1 (2005), to Basell Poliolefine Italia S.P.A.
[3] A.K. Karbasi, T. Leinonen, P. Sormunen, EP Patent 0,627,449 A1 (1994), to Neste Oy.
[4] J. Koskinen, P. Jokinen, WO Patent 93/19100 (1993), to Neste Oy.
[5] G. Ertl, H. Knözinger, J. Weitkamp, Preparation of Solid Catalysts, VCH, Weinheim, 1999.
[6] J.J.A. Dusseault, C.C. Hsu, J. Macromol. Sci. Rev. Macromol. Chem. Phys. C 33 (2) (1993) 103.
[7] G. Leofanti, M. Padovan, G. Tozzola, B. Venturelli, Catal. Today 41 (1998) 207.
[8] J.W. Niemantsverdriet, Spectsoscopy in Catalysis, An Introduction, VCH, Weinheim, 1995.
[9] L. Brambilla, G. Zerbi, S. Nascetti, F. Piemontesi, G. Moroni, Macromol. Symp. 213 (2004) 287.
[10] G.G. Arzoumanidis, N.M. Karayannis, Stud. Surf. Sci. Catal. 56 (1990) 147.
[11] T. Leinonen, P. Denifl, EP Patent 1,273,595 A1 (2003), to Borealis Technology Oy.
[12] M. Abboud, P. Denifl, K.-H. Reichert, Macromol. Mater. Eng. 290 (2005) 1220.
[13] V. Di Noto, S. Bresadola, Macromol. Chem. Phys. 197 (1996) 3827.
[14] E.E. Kis, G.A. Lomic, B.D. Skrbic, D.M. Stoiljkovic, E.M. Dinkova, Acta Period. Technol. 28 (1997) 123.
[15] G. Socrates, Infrared, Raman Characteristic Group Frequencies, Tables and Charts, 3rd ed., Wiley, England, 2004.
[16] C.R. Tewell, UV–Raman spectroscopy, X-ray photoelectron spectroscopy and temperature programmed desorption studies of model bulk heterogeneous catalysts, Dissertation, 2002.
[17] M. Hosaka, I. Nishiyama, US Patent 6,228,793 B1 (2001), to Toho Titanium Co.
[18] M. Vittadello, P.E. Stallworth, F.M. Alamgir, S. Suarez, S. Abbrent, C.M. Drain, V. Di Noto, S.G. Greenbaum, Inorg. Chim. Acta 359 (2006) 2513.
[19] V. Di Noto, S. Bresadola, R. Zannetti, M. Viviani, Zeit. Kristallogr. 201 (1992) 161.
[20] V. Di Noto, R. Zannetti, S. Bresadola, A. Marigo, C. Marega, Inorg. Chim. Acta 190 (1991) 279.
[21] V. Di Noto, L. Pavanello, M. Viviani, G. Storti, S. Bresadola, Thermochim. Acta 189 (1991) 223.
[22] M. Chang, X. Liu, P.J. Nelson, G.R. Munzing, T.A. Gegan, Y.V. Kissin, J. Catal. 239 (2006) 347.